Published in final edited form as:
Neuroscience. 2012 November 8; 224: 160–171. doi:10.1016/j.neuroscience.2012.08.023.

The ubiquitin ligase FBG1 promotes the degradation of the disease-linked protein torsinA through the ubiquitin proteasome pathway and macroautophagy

Kara L Gordon[a], **Kevin A Glenn**[b,c], **Nicole Bode**[d], **Hsiang M Wen**[c], **Henry L Paulson**[e], and **Pedro Gonzalez-Alegre**[a,d]

Kara L Gordon: kara-gordon@uiowa.edu; Kevin A Glenn: kevin-glenn@uiowa.edu; Nicole Bode: nicole-bode@uiowa.edu; Hsiang M Wen: hsiang-wen@uiowa.edu; Henry L Paulson: henryp@umich.edu; Pedro Gonzalez-Alegre: pedro-gonzalez-alegre@uiowa.edu

[a]Graduate Program of Neuroscience, University of Iowa, Iowa City, IA 52242 USA

[b]Veterans Administration Hospital, Iowa City, IA 52242 USA

[c]Department of Internal Medicine, Carver College of Medicine, University of Iowa, Iowa City, IA 52242 USA

[d]Department of Neurology, Carver College of Medicine, The University of Iowa, Iowa City, IA 52242 USA

[e]Department of Neurology, University of Michigan, Ann Arbor, MI 48109 USA

Abstract

DYT1 dystonia is a dominantly inherited, disabling neurological disorder with low penetrance that is caused by the deletion of a glutamic acid (ΔE) in the protein torsinA. We previously showed that torsinA(wt) is degraded through macroautophagy while torsinA(ΔE) is targeted to the ubiquitin proteasome pathway (UPP). The different catabolism of torsinA(wt) and (ΔE) potentially modulates torsinA(wt):torsinA(ΔE) stoichiometry. Therefore, gaining a mechanistic understanding on how the protein quality control machinery clears torsinA(ΔE) in neurons may uncover important regulatory steps in disease pathogenesis. Here, we asked whether FBG1, a ubiquitin ligase known to degrade neuronal glycoproteins, is implicated in the degradation of torsinA(ΔE) by the UPP. In a first set of studies completed in cultured cells, we show that FBG1 interacts with and influences the steady-state levels of torsinA(wt) and (ΔE). Interestingly, FBG1 achieves this effect promoting the degradation of torsinA not only through the UPP, but also by macroautophagy. To determine the potential clinical significance of these findings, we asked if eliminating expression of *Fbg1* triggers a motor phenotype in torsinA(ΔE) knock in mice, a model of non-manifesting DYT1 mutation carriers. We detected differences in spontaneous locomotion between aged torsinA(ΔE) knock in-*Fbg1* knock out and control mice. Furthermore, neuronal levels of torsinA were unaltered in *Fbg1* null mice, indicating that redundant systems likely compensate *in vivo* for the absence of this ubiquitin ligase. In summary, our studies support a non-

Address correspondence to: Pedro Gonzalez-Alegre, MD, PhD, Department of Neurology, Carver College of Medicine, The University of Iowa, 3111A MERF, 375 Newton Road, Iowa City, IA 52242 USA, Phone: +1 319 335 9178, Fax: +1 319 335 9517, pedro-gonzalez-alegre@uiowa.edu.

The authors declare no conflicts of interest.

essential role for FBG1 on the degradation of torsinA and uncover a novel link of FBG1 to the autophagy pathway.

Keywords

TorsinA; DYT1 dystonia; FBG1; ubiquitin proteasome pathway; autophagy; protein degradation

DYT1 dystonia is a dominantly inherited brain disorder characterized by involuntary muscle twisting that leads to abnormal postures (Tarsy and Simon, 2006). DYT1 is caused by a GAG deletion in the gene *TOR1A* (Ozelius et al., 1997). This dominant mutation exhibits low penetrance, as only about a third of mutation carriers develop symptoms (Tarsy and Simon, 2006). Therefore, the identification of mechanisms that regulate disease pathogenesis might uncover important clues on how penetrance is determined.

TOR1A encodes torsinA, an endoplasmic-reticulum (ER) resident protein (Hewett et al., 2000, Kustedjo et al., 2000) that belongs to the family of AAA+ ATPases (Ozelius et al., 1997). The DYT1 mutation translates into the deletion of a glutamic acid residue in torsinA, (torsinA(ΔE)) (Ozelius et al., 1997). Both forms of torsinA, wild type (wt) and (ΔE), are co-translationally imported into the ER and do not progress through the secretory pathway (Hewett et al., 2000, Callan et al., 2007). However, torsinA(wt) is preferentially located in ER sheets (Vander Heyden et al., 2011), while the mutant form concentrates in the nuclear envelope (NE) (Gonzalez-Alegre and Paulson, 2004, Goodchild and Dauer, 2004, Naismith et al., 2004). Findings from different laboratories suggest that torsinA(ΔE) acts through a dominant negative effect over torsinA(wt), through a toxic gain of function, or both (Goodchild and Dauer, 2004, Koh et al., 2004, Torres et al., 2004, Gonzalez-Alegre et al., 2005, Misbahuddin et al., 2005, Hewett et al., 2007, Hewett et al., 2008, Nery et al., 2008, O'Farrell et al., 2009). Whatever the final mechanism of disease pathogenesis proves to be, a substantial amount of experimental evidence indicates that torsinA(ΔE) expression is deleterious for central neurons. Therefore, the cellular mechanisms that regulate the levels of torsinA(ΔE) could play an important modulatory role on disease pathogenesis.

A critical process in the pathogenesis of many neurological diseases, such as Parkinson's or Alzheimer's disease, is the neuronal ability to clear disease-linked proteins (Nedelsky et al., 2008). This is also probably true for DYT1 dystonia. TorsinA is a very stable protein normally recycled through the non-selective process of macroautophagy (hereafter referred to as autophagy) (Giles et al., 2008, Gordon and Gonzalez-Alegre, 2008). The (ΔE) mutation, however, redirects this protein to the ubiquitin proteasome pathway (UPP) through ER-associated degradation (ERAD) (Giles et al., 2008, Gordon and Gonzalez-Alegre, 2008) significantly shortening its half-life. This results in a reduction of the steady-state levels of torsinA in DYT1 knock in (KI) mice and in human DYT1 fibroblasts despite similar transcript expression for both alleles (Goodchild et al., 2005). Consequently, any biological event that impairs the rapid clearance of torsinA(ΔE) by the UPP would increase its levels, potentially exacerbating the pathogenic process in DYT1.

A first step to understand the mechanism underlying the rapid clearance of torsinA(ΔE) is to identify key elements of this process. Protein degradation by the UPP is selective, requiring the identification of specific substrates for their ubiquitination and subsequent degradation. Ubiquitin ligases are the components of this pathway that provide substrate selectivity (Ciechanover and Brundin, 2003). They attach a poly-ubiquitin tag to specific proteins that facilitates their recognition as a degradation substrate by the proteasome. We hypothesize that the ubiquitin ligases that target torsinA(ΔE) to the UPP play a key protective role in lowering the steady-state levels of this protein in the DYT1 brain.

Of the several hundred ubiquitin ligases in the human proteome (Ciechanover and Brundin, 2003), F-box/G-domain protein 1 (FBG1) is an excellent candidate to catalyze the degradation of torsinA(ΔE). FBG1 is the substrate-binding component of a multisubunit SKP, Cullin, F-box (SCF) E3 ubiquitin protein ligase (Erhardt et al., 1998, Yoshida et al., 2002). FBG1 is preferentially expressed in neurons and binds ER glycoproteins that contain high mannose N-linked glycans targeting them for degradation through ERAD (Yoshida et al., 2002, Glenn et al., 2008). Examples of FBG1 substrates are pre-integrin β1, CFTR-ΔF508, SHPS-1, NR1 and NR2A subunits of the NMDA receptor, and BACE (Yoshida et al., 2002, Murai-Takebe et al., 2004, Kato et al., 2005, Nelson et al., 2006, Gong et al., 2010). Because torsinA(ΔE) is pathogenic in central neurons, is modified by two high mannose glycan groups (Hewett et al., 2000, Kustedjo et al., 2000) and is rapidly degraded through ERAD (Giles et al., 2008, Gordon and Gonzalez-Alegre, 2008), we hypothesized that FBG1 participates in the degradation of torsinA(ΔE). To test this hypothesis, we designed cell-based experiments to determine if FBG1 interacts with torsinA(ΔE) and modulates its steady-state levels. Subsequently, we explored the potential clinical significance of this process by studying if FBG1 expression modulates motor phenotypes in a mouse model of DYT1 dystonia.

1. Experimental procedures

1.1 Cell culture and transfection

PC6.3 cells were grown and maintained in RPMI with 10% HS and 5% FBS (all from Gibo, Grand Island, NY, USA), and differentiated in RPMI with 2% HS and 1% FBS with 100 ng/ml nerve growth factor (NGF) as described (Gordon et al., 2011). TorsinA(wt) and (ΔE) (Gonzalez-Alegre and Paulson, 2004) and HA-FBG1 inducible PC6.3 cells (Wen et al., 2010) were induced with doxycycline at 1.5 μg/ml as described (Gordon et al., 2011). Cos7 and HEK293 cells were grown and maintained in DMEM (Gibco) with 10% FBS as described (Gordon and Gonzalez-Alegre, 2008). These cell lines were transiently transfected using LIPOfectamine 2000 or Lipofectamine PLUS (Invitrogen, Grand Island, NY, USA) according to manufacturer's protocol. Hep-G2 (human liver, hepatocellular carcinoma) cells obtained from ATCC were grown and maintained in Eagle's MEM (Sigma, St. Louis, MO, USA), 10% FCS, 2 mM L-glutamine, 1% non-essential amino acids, and 1% NA pyruvate. shRNA constructs were transfected into HepG2 cells using Lipofectamine PLUS (Invitrogen). Cells were treated with 3μg/mL puromycin for 10 days to eliminate non-transfected cells. Clones were selected and allowed to expand.

1.2. Plasmid vectors and transfections

Transient transfection was performed using the pCDNA3.1 torsinA(wt) and torsinA(ΔE) constructs previously described (Gonzalez-Alegre et al., 2003), pFLAG-CMV-6b with FBG1, FBG1(ΔN), FBG2, FBG3 or alkaline phosphatase (AP) as a control (Glenn et al., 2008). The FLAG-FBG1(ΔN) construct has the N-terminal portion consisting of both the PEST and F-box domains removed. Co-transfection was performed at a 2:1 ratio of FBG1 to torsinA. shRNA expression plasmid #4306 (Sigma) containing the sequence "CCGGCACCGTTAAGCTACTGTCCGACTCGAGTCGGACAGTAGCTTAACGGTGTTTTT" to silence FBG1 were used to make HepG2 clones. As previously described (Gordon and Gonzalez-Alegre, 2008), autophagy and proteasomal inhibition were achieved by adding 10 mM 3-Methyladenine (3-MA) (Sigma) or 10 μM lactacystin (Calbiochem, Billerica, MA, USA) to the media as indicated. Cycloheximide (Sigma) was used at 10 μM in PC6.3 cells to inhibit protein synthesis.

1.3. Western Blot

Samples were harvested in Laemmli buffer with 200 mm DTT (Research Products International, Mt. Prospect, IL, USA), sonicated, and boiled 5 min prior to loading on 12% SDS-PAGE gels and transfer to PVDF membrane. Western blot analysis was performed and protein signal was quantified using Image J (NIH. Bethesda, MD, USA). Control samples for each set were assigned a relative density of 1 and density of experimental samples were calculated compared to control. All samples were then normalized to tubulin loading control. Quantification data is shown as % western blot signal from at least 3 replicates with standard error of the mean (SEM). Statistical analysis was performed as appropriate using Students independent t-test, one-way or two-way ANOVA followed by Tukey's post hoc test ($p \leq 0.05$). Antibodies used were torsinA and Fbx06 (for FBG2) (Abcam, Cambridge, MA, USA), TA913 (Gordon and Gonzalez-Alegre, 2008), FBG1 (FBX02) (Glenn et al., 2008), tubulin, GAPDH and FLAG (polyclonal or M5) (Sigma), ubiquitin (Dako, Carpinteria, CA, USA), GFP (Roche, Indianapolis, IN, USA), and THE HA (Genscript, Piscataway, NJ, USA). Horseradish Peroxidase (HRP) conjugated secondary antibodies (Jackson ImmunoResearch Laboratories, West Grove, PA, USA) were used along with Western Lightning ECL (Pierce, Rockford, IL, USA) reagents to visualize blots.

1.4. Immunoprecipitation

GST-pulldown experiments were performed as described (Glenn et al., 2008). Briefly, lysates prepared from doxycycline inducible PC6.3 cells overexpressing torsinA(wt) or torsinA(ΔE) were incubated with purified GST-FBG1 fusion protein and 15 ul of Glutathione-Sepharose-4B beads (GE Healthcare, Piscataway, NJ, USA) for 30 min at room temperature. The beads were then transferred to Micro-Spin columns (Pierce), washed 4 times with FLAG lysis buffer, and eluted with Laemmli buffer at room temperature for 15 min. Bound proteins were resolved by SDS-PAGE. For co-immunoprecipitation experiments, HEK293 cells in 10 cm dishes were transiently co-transfected with FLAG-FBG1 or FLAG-FBG3 and torsinA(wt) or (ΔE). Lysates were collected in FLAG lysis buffer with protease inhibitor cocktail (Roche). Lysates were centrifuged for 20 min at 12,000 rpm following incubation on ice. Supernatant was removed and immunoprecipitation with anti-FLAG M2 affinity gel (Sigma) was performed. The beads were transferred to Micro-Spin columns (Pierce), washed 4 times with FLAG lysis buffer, and eluted with Laemmli buffer without DTT at room temperature for 15 min. Eluted proteins were resolved by SDS-PAGE to determine interacting proteins.

1.5. Confocal microscopy

We generated plasmid vectors expressing fluorescently-tagged torsinA(wt and ΔE) and FBG1 using In-Fusion Cloning (Clontech, Mountain View, CA, USA). Untagged torsinA was inserted into pAmCyan-N1 (Clontech) (in-frame C-terminal fusion after eliminating the stop codon, as N-terminal tag could alter import into ER) and FBG1 into pZsYellow1-C1 (Clontech) (N-terminal fusion after mutating the initial ATG). Sequence was verified and western blot performed to confirm expression of the fusion protein at the appropriate molecular weight. For colocalization studies, PC6.3 cells were transiently co-transfected as above. Live cells were visualized and images collected 30 hours after transfection using a Zeiss 510 Confocal microscope at the Central Microscopy Research Facility (CMRF) (University of Iowa, Iowa City, IA, USA). Images were pseudocolored green for torsinA-AmCyan signal or red for ZsYellow-FBG1 signal and merged.

1.6. Animals

Tor1a KI mice (Goodchild et al., 2005), were crossed with *Fbg1* knock-out (KO) mice (also known as *Fbx2*) (Nelson et al., 2007). 123 mice of 6 genotypes were generated. Mice were

housed in controlled temperature rooms with 12 hr light and dark cycles with food and water provided *ad libitum*. All experimental protocols were approved by the University of Iowa Animal Care and Use Committee (ACURF #0609196). Weights were recorded each month from 1–18 months of age. Mendelian ratios of birth were determined as well as survival of the mice up to 18 months of age. Weights were statistically analyzed by repeated measures ANOVA ($p \leq 0.05$) and survival by the Kaplan-Meier method using Prism (GraphPad Software, La Jolla, CA) statistical software.

1.7. Behavioral Analysis

Test of spontaneous locomotion was performed by placing 4 mice simultaneously in an open field arena with 4 separated 25 cm × 25 cm quadrants after acclimation to the room as previously described (Martin et al., 2011). The movement of the mice was recorded using a ceiling mounted video camera connected to an automated tracking system (Viewpoint Videotrack, Lyon, France) used to collect the total distance traveled by each mouse during a 90 min trial with data collected in 5 min bins during the light cycle at similar times each day. Locomotor testing was performed initially at 3 months of age and repeated at 6, 9, 12, 15, and 18 months. Statistical analysis was performed for all surviving animals on 6–18 month tests using repeated measures ANOVA with Bonferroni post-hoc tests ($p \leq 0.05$).

Mice were tested on an accelerating rotarod at 18 months of age. Mice were acclimated to the rotarod (model 47 600 Ugo Basile, Milan, Italy) at 4 rpm for 3 min followed by 2 min with acceleration from 4 rpm to 19 rpm. For the trials, an accelerating paradigm was used with acceleration from 4 rpm to 40 rpm over 300 sec with max trial duration 500 sec. Latency to fall from rod was recorded. Mice that rode the rotating rod during the trial for 3 revolutions without walking were removed due to inactivity. Mice were tested for 3 days with 3 trials per day and at least 20 min rest between each trial. For analysis, all trials were averaged or the 3 trials per day were averaged to determine an average latency to fall for each genotype. Statistical analysis was performed using two-way ANOVA or repeated measures ANOVA, respectively, with Bonferroni post-hoc test ($p \leq 0.05$).

1.8. Brain analysis

Mice were sacrificed at 18 months after final behavioral analysis. Transcardial perfusion was performed with ice cold 0.9% NaCl for protein analysis or fixed with 4% PFA for histological analysis. Brains were excised from the cranial cavity and either flash frozen and stored at −80°C for protein or post-fixed overnight and stored at 4°C in 30% sucrose. For protein analysis by western blotting, tissue was homogenized in RIPA lysis buffer with protease inhibitor cocktail (Roche) and 10 mM N-ethylmaleimide (NEM) (Sigma) followed by centrifugation at 4000 rpm for 15 min at 4°C and removal of supernatant. Approximate concentrations were determined using a filter paper concentration assay of samples compared to known BSA standards. 40–50 μg of protein was diluted up to 10 μl in RIPA buffer followed by addition of 10 μl 2X Laemmli buffer with 200 mM DTT. Samples were analyzed by western blot as described above.

PFA-fixed brain tissue was cut using a sledge microtome (Leica, Buffalo Grove, IL, USA) for 40 micron sections and stored as floating sections in cryostorage solution at 4°C. Brains from 4 animals per genotype were cut and 8 slices of similar location from the frontal lobe to post striatal area were chosen for staining. Slices were rinsed in PBS, then mounted onto slides for Hematoxylin and Eosin (H&E) staining. Briefly, slices rehydrated in distilled water were dipped in solutions in the following order: staining in Hematoxylin (Harris formula, Surgipath, Buffalo Grove, IL, USA), distilled water rinse, decolorization in acid alcohol (0.5% HCl), distilled water rinse, 1.36% Lithium carbonate solution, distilled water rinse, 80% ethanol, stained in eosin containing phloxine, followed by dehydration in 2

changes of 95% alcohol, 3 changes of 100%, then 3 changes of Xylenes and coverslipped using Cytoseal 60 (Thermo Scientific, Rockford, IL, USA) mounting medium. Slices were viewed and pictures captured on an Olympus BX-51 microscope with DP-70 camera (Olympus, Center Valley PA, USA) (CMRF).

2. Results

2.1. TorsinA-FBG1 interactions

In a first set of experiments, we investigated if FBG1 and torsinA interact, as predicted by the high-mannose glycan-binding properties of FBG1 and the presence of 2 high-mannose tags in torsinA. We induced expression of torsinA(wt) and torsinA(ΔE) with doxycycline in previously reported PC6.3 inducible cell lines (Gonzalez-Alegre and Paulson, 2004) and obtained non-denaturing lysates. The lysates were incubated with recombinant GST-FBG1 (or GST control) to assess for a direct interaction as has been previously used to identify FBG1-interacting proteins (Nelson et al., 2006, Glenn et al., 2008). Both torsinA(wt) and torsinA(ΔE) interacted with GST-FBG1, but not with GST control (Figure 1A). To further investigate the interaction between FBG1 and torsinA(ΔE), cells were transiently transfected with FLAG-FBG1 and torsinA(wt) or (ΔE), obtaining non-denaturing lysates 48 hrs later and followed an immunoprecipitation protocol with anti-FLAG affinity gel. This approach confirmed the presence of torsinA-FBG1 interactions (Figure 1B). To determine if the interaction was due to the glycan- binding property of FBG1, we included a control transfected with FLAG-FBG3, the only member of the FBG family that does not bind glycans (Glenn et al., 2008). These experiments did not show any interaction between FBG3 and torsinA (Figure 1B). Finally, to evaluate if FBG1 and torsinA co-localize, we expressed torsinA-AmCyan and ZsYellow-FBG1 expressing vectors into PC6.3 cells followed by confocal microscopy. These experiments showed areas of co-localization, but also non-overlapping signal (Figure 1C). This is consistent with the different subcellular localization of both proteins under normal conditions (ER and cytosol), and co-localization once torsinA has been retrotranslocated for degradation.

2.2. FBG1 influences steady state levels of torsinA

Next, we asked if FBG1 expression alters the steady-state levels of torsinA. We transiently co-expressed torsinA(wt) or torsinA(ΔE) with FLAG-FBG1 or a control plasmid in Cos7 cells. Western blot analysis of torsinA expression 48 hrs later showed that overexpression of FLAG-FBG1, but not the control plasmid, reduced levels of torsinA(wt) and torsinA(ΔE) (Figure 2A). To confirm these findings in a neuronal model, we used NGF-differentiated PC6.3 cells. Co-expression of FLAG-FBG1 and torsinA(ΔE) led to significant reduction in torsinA(ΔE) levels 48 hrs after transfection (Figure 2C), consistent with our results in Cos7 cells. A potential concern with transient transfection is that it leads to very high levels of expression, which we have shown might lead to the recruitment of alternative protein degradation pathways (Gordon and Gonzalez-Alegre, 2008). To use a more physiological system, we employed an inducible PC6.3 cell system that expresses HA-FBG1 upon addition of doxycycline to the media. PC6.3 cells express endogenous torsinA. Thus, we asked if inducing HA-FBG1 expression lowered steady-state levels of endogenous rat torsinA. HA-FBG1 expression was induced with doxycycline. Because the half-life of torsinA is ~80 hrs (Giles et al., 2008), translational inhibition with cycloheximide was used to facilitate the detection of changes in protein levels. HA-FBG1 expression led to a small but significant reduction in the levels of endogenous torsinA (see later Figure 3B). Finally, Hep-G2 cells express high endogenous levels of FBG1 and torsinA. We used this cell line to evaluate the consequences of acute suppression of FBG1 expression through RNA interference on torsinA. Hep-G2 cells were transfected with the shRNA-expression plasmid #4306 targeting endogenous FBG1. Expression of endogenous FBG1 and torsinA were

measured by western blotting. We found, in multiple clones, that suppressing expression of endogenous FBG1 proportionally increased levels of torsinA (Figure 2E and not shown). Collectively, these experiments indicate that FBG1 expression modulates the steady-state levels of torsinA in cultured cells.

FBG1 has been shown to function as a canonical SCF complex (Yoshida et al., 2002) but also independent of CUL1 (Nelson et al., 2007, Yoshida et al., 2007). As deletion of the F-box domain abolishes its interaction with other components of the SCF complex (Bai et al., 1996), we transiently co-expressed torsinA with an FBG1 construct lacking the N-terminal domain (FLAG-FBG1(ΔN)) in Cos7 cells to investigate SCF-dependent or independent activities of FBG1 on torsinA degradation. As shown in Figure 2B, FLAG-FBG1(ΔN) no longer altered torsinA(wt) levels. Surprisingly, FLAG-FBG1(ΔN) still reduced the levels of torsinA(ΔE) (Figure 2B), consistent with an SCF-independent activity. These results were also observed in PC6.3 cells (Figure 2D). The apparent ability of FBG1 to modulate levels of torsinA(ΔE), but not torsinA(wt), through both SCF-dependent and independent pathways indicates that there are mechanistic differences in how FBG1 influences torsinA(wt) and (ΔE) expression.

2.3. FBG1 promotes torsinA degradation through different degradation pathways

The studies above showed that FBG1 interacts with torsinA and influences its expression levels. Next, we asked if FBG1 modulates torsinA levels through the proteasomal or autophagic pathways. PC6.3 cells were co-transfected with FLAG-FBG1, FLAG-FBG1(ΔN) or control FLAG-AP and torsinA(ΔE). 36 hrs later, 10 μM lactacystin or 10 mM 3-MA were added for 12 hrs to inhibit the proteasome or autophagy, respectively. When co-expressed with FLAG-FBG1, the reduction in levels of torsinA(ΔE) was rescued by both proteasomal and autophagy inhibition (Figure 3A). This result suggests FBG1 has the ability to promote its degradation through both proteasomal and autophagic pathways. When co-expressed with FLAG-FBG1(ΔN), only proteasomal inhibition restored torsinA(ΔE) levels (Figure 3A). The partial rescue of torsinA(ΔE) levels by autophagy and proteasomal inhibition in the presence of FBG1, but only upon proteasomal inhibition with FBG1(ΔN), suggests that the N-terminal domain provides FBG1 with flexibility to target substrates to autophagy.

We initially hypothesized that FBG1 would function through the UPP, but we found that it also reduces levels of torsinA(wt) (Figure 2A), which is normally recycled through autophagy. Therefore, we used torsinA(wt) to confirm that FBG1 targets substrates for autophagic degradation, and not only to the UPP. PC6.3 cells that inducibly express HA-FBG1 were treated 24 hrs after induction with 10 μM lactacystin or 10 mM 3-MA in addition to cycloheximide for 24 hrs. Inducing expression of HA-FBG1 for 48 hrs reduced levels of endogenous torsinA. In contrast to torsinA(ΔE), only autophagy inhibition, but not proteasomal inhibition, rescued this effect (Figure 3B). These results with endogenous torsinA confirm the ability of FBG1 to target torsinA for degradation through the autophagy pathway.

2.4. Loss of FBG1 modifies motor phenotype in *Tor1a*$^{+/\Delta E}$ mice

Based on our tissue culture experiments, we hypothesized that FBG1 modulates the clearance of neuronal torsinA *in vivo*. As a consequence, loss of FBG1 function could lead to increased levels of torsinA(ΔE) and trigger or exacerbate DYT1-linked phenotypes. To test this hypothesis, we performed experiments using a DYT1 mouse model.

Tor1a$^{+/\Delta E}$ KI mice, developed by Dauer and colleagues (Goodchild et al., 2005), do not exhibit significant motor abnormalities and are regarded as a model of non-manifesting

DYT1-mutation carriers. Thus, this model is well-suited to identify genetic or environmental triggers of DYT1 phenotypes. We hypothesized that eliminating expression of *Fbg1* in this model would lead to increased levels of torsinA(ΔE) and, as a result, possible motor dysfunction. *Fbg1* null mice were previously described by Paulson and colleagues and do not exhibit motor dysfunction or other overt developmental abnormalities (Nelson et al., 2007). To test our hypothesis, we bred $Tor1a^{+/\Delta E}$ mice with $Fbg1^{+/-}$ mice. Mendelian ratios of the 6 genotypes generated were as expected (Figure 4A). We focused our studies on the $Fbg1^{+/+}$ and $Fbg1^{-/-}$ mice as total loss of FBG1 would be most likely to exacerbate the phenotypes examined. Genotype did not significantly influence the weight or survival of the animals out to 18 months (Figures 4B–D), allowing evaluation of motor function.

Upon repeated visual inspection of in-cage behavior over time, we found no abnormal movements suggestive of dystonia. Several mouse models of DYT1 have demonstrated age-dependent hyperactivity in the open field test (Dang et al., 2005, Shashidharan et al., 2005, Grundmann et al., 2007). Therefore, we performed tests of spontaneous locomotion in an open field at 3, 6, 9, 12, 15, and 18 months of age to ensure detection of any age-dependent motor deficits resulting from the ΔE mutation and exacerbated by the loss of FBG1. We evaluated total distance traveled during 90 min trials at each time point to assess spontaneous locomotion. Analysis of distance traveled over time using repeated measures ANOVA showed a significant effect of time and genotype, but no interaction between time and genotype (Figure 5A). Surprisingly, these studies suggested reduced locomotion, not hyperactivity. Analysis of individual time points identified significant differences only in aged mice, suggesting hypoactive locomotion caused by the DYT1 mutation and loss of FBG1 (Figure 5A).

We evaluated motor performance on the accelerating rotarod at 18 months of age, which has been reported to be abnormal in a transgenic DYT1 mouse model (Sharma et al., 2005). The average latency for each group of mice to fall from the accelerating rotarod is shown in Figure 5B. Interestingly, on the $Fbg1^{+/+}$ background, $Tor1a^{+/\Delta E}$ mice exhibit impaired ability to remain on the rotarod. Unexpectedly, loss of FBG1 rescues this phenotype. To determine if this deficit represents impairment of motor performance or a motor learning deficit (failure to learn over consecutive trials), we also analyzed the daily performance on the rotarod over the 3 consecutive days. This analysis showed the presence of defective performance in $Fbg1^{+/+}$-$Tor1a^{+/\Delta E}$ mice from day 1, indicating defective performance (Figure 5C).

2.5. Loss of FBG1 does not alter neuronal torsinA expression levels

We examined the brains of the animals by H&E staining to search for gross changes in brain structure that could influence protein expression. As expected based on previous reports (Dang et al., 2005, Nelson et al., 2007), *Tor1a* KI and *Fbg1* null mice did not exhibit gross neuroanatomical abnormalities (not shown). The same was true for the genetic cross (not shown). Subsequently, we homogenized whole brain and completed western blot analysis for torsinA and FBG1 expression. As previously reported (Goodchild et al., 2005), $Tor1a^{+/\Delta E}$ mice have lower torsinA levels than $Tor1a^{+/+}$ animals. However, the levels of torsinA were not influenced by the presence or absence of FBG1 (Figure 6A). We felt this finding might derive from the presence of functional redundancy. Of the other 5 members of the FBG family, FBG2 has the closest glycoprotein binding pattern to FBG1 (Glenn et al., 2008). To test if FBG2 could be functionally redundant with FBG1, we transiently transfected FLAG-FBG2, FLAG-FBG1, or FLAG-AP control with torsinA(wt) or (ΔE) in Cos7 cells. These experiments showed that FBG2 overexpression, similar to FBG1, reduces levels of torsinA(wt) and (ΔE) compared to control plasmid (Figure 6B). Western blotting of brain lysates obtained from the mice in Figure 6A demonstrated expression of this ubiquitin ligase in brain tissue, although with variable levels among different animals

independent of their genotype (Figure 6C). While not conclusive, these experiments are consistent with the possibility that FBG2, and perhaps other ubiquitin ligases, could compensate for the congenital loss of FBG1 *in vivo*.

3. Discussion

In this study, we investigated the potential influence of the ubiquitin ligase component FBG1 on torsinA expression in cultured cells and on DYT1 phenotypes *in vivo*. We found that FBG1 binds torsinA(ΔE) and torsinA(wt) and influences their steady-state levels through different mechanisms, indicating its participation in torsinA degradation. However, genetic ablation of FBG1 expression in a mouse model of DYT1 does not alter brain levels of torsinA. Altogether, these results are consistent with the participation of FBG1 in the degradation of torsinA through a non-essential and likely redundant process. In addition, our studies support previous reports that showed significant versatility of FBG1 interactions and function. Based on versatility provided by its N-terminal domain, we show that FBG1 assists in the degradation of torsinA through the UPP and autophagy.

3.1. Redundant systems likely compensate for the absence of FBG1 to degrade torsinA

We show that FBG1 modulates torsinA degradation in different cell systems. Although over-expression systems can produce artifactual results, we found that increased expression and silencing of FBG1 influenced levels of endogenous torsinA in the opposite direction. The findings presented here using over-expressed and endogenous torsinA strongly indicate that FBG1 acts on both forms of torsinA. This is not surprising, as FBG1 is known to participate in the degradation of other ER high-mannose glycoproteins, and both FBG1 and torsinA are expressed in central neurons. Thus, FBG1 is the first identified protein that participates in the catabolism of torsinA. Future studies will expand this finding to identify additional down- and upstream components of this process.

Elimination of *Fbg1* in *Tor1a* KI mice did not trigger motor dysfunction or alter the levels of torsinA. In fact, the abnormal performance on the rotarod in aged $Tor1a^{+/\Delta E}$ mice was rescued by the loss of FBG1. Several possibilities could explain why the loss of FBG1 fails to cause motor dysfunction or increase torsinA levels in vivo. For example, the presence of redundant proteins, such as the functionally similar FBG2, may compensate for the absence of FBG1 to ensure proper degradation of torsinA(ΔE). Other ER ubiquitin ligases, such as HRD1 (Groisman et al., 2006), may also recognize and target torsinA for degradation. The absence of redundancy in our cell models is not surprising as acute overexpression or silencing is less likely to allow the development of efficient compensatory changes. In contrast, the developmental absence of FBG1 expression in *Fbg1* KO mice is more likely to allow the development of redundant systems to maintain cellular homeostasis. Future experiments could address the consequences of silencing expression of FBG2 and other ubiquitin ligases that potentially provide a compensatory mechanism for the degradation of torsinA(ΔE) in *Fbg1* null mice.

3.2. FBG1 is a versatile protein linked to proteasomal and autophagic degradation

While the main goal of this work was to determine if FBG1 participates in the degradation of torsinA and influences DYT1 phenotypes, our experiments yielded interesting findings on FBG1. Previous reports indicate that FBG1 not only functions as a component of an SCF complex, but also independently (Nelson et al., 2007, Yoshida et al., 2007). In addition to providing additional experimental support to the SCF-independent function of FBG1, we show that this versatile ubiquitin ligase has the capacity to direct targets for degradation by different catabolic routes.

How does FBG1 achieve such functional flexibility? Nelson et al. (2006) showed that FBG1 participates in glycoprotein ubiquitination through an interaction with the co-chaperone/E3 ligase CHIP mediated by the N-terminal PEST domain of FBG1. It is uncertain if this cooperative action between FBG1 and CHIP occurs in an SCF-dependent or independent manner. Furthermore, FBG1 forms heterodimers with SKP1 reducing glycoprotein aggregation (Yoshida et al., 2007). A recent report highlighted promiscuous interactions of FBG1 with different adaptor proteins through its N-terminal domain that potentially modulate substrate selection (Wen et al., 2010). We observed an effect of FBG1 when lacking its N-terminal domain (both the F-box and PEST domains) on torsinA levels which further suggests the presence of SCF-independent and CHIP-independent mechanisms. Thus, the flexibility in protein-protein interactions conferred by the N-terminal domain of FBG1 likely translates into functional versatility in handling substrates. Collectively, reports to date suggest that FBG1 is a non-conventional F-box protein that likely plays a wider role in protein degradation than its known role in SCF-mediated ubiquitination and degradation of ER glycoproteins by the UPP.

Our findings show that FBG1 facilitates the clearance of torsinA by the two main ER degradation pathways, the UPP and autophagy. Functional links between the UPP and autophagy are being increasingly uncovered at different levels (Bernales et al., 2006, Pandey et al., 2007). Parkin, an ubiquitin ligase mutated in inherited Parkinson's disease, ubiquitinates proteins for degradation by both the proteasome and autophagy (Shimura et al., 2000, Olzmann et al., 2007). The experiments reported here suggest that FBG1 shares the ability of targeting substrates to both pathways. FBG1 participates in the proteasomal degradation of ER glycoproteins such as CFTR-Δ508 (Yoshida et al., 2002), BACE (Gong et al., 2010) and NMDA receptor subunits (Kato et al., 2005). However, its link to autophagy is novel. Yoshida et al. (2007) speculated about a possible link of FBG1 and autophagy based on the effect of FBG1-SKP1 heterodimers on protein aggregates. Our results provide experimental support for this hypothesis. We found that the N-terminal domain of FBG1 is necessary for its actions through autophagy (Figure 3A). It is possible that the regulated interactions with other proteins mediated by the N-terminal domain of FBG1 help to specify the catabolic route for specific substrates depending on their biochemical properties and cellular environment. For instance, CHIP binds FBG1 through the N-terminal domain (Nelson et al., 2006). A recent report indicates that CHIP cooperates with BAG-3 in a process termed chaperone-assisted selective autophagy (CASA) (Arndt et al., 2010). BAG-3 is engaged in the autophagic degradation of several neuronal disease associated proteins (Carra et al., 2008, Crippa et al., 2010, Gamerdinger et al., 2011). We found that deletion of the N-terminal domain of FBG1, which should prevent its interaction with CHIP and participation in CASA, abolishes its ability to target torsinA to autophagy. Thus, FBG1 might interact with CHIP and BAG-3 to clear torsinA through CASA. Whatever the mechanism by which FBG1 regulates torsinA levels proves to be, it is increasingly clear that it does not simply act as an SCF E3 ligase to direct glycoproteins for ERAD. Future experiments will be designed to expand our knowledge of the link between FBG1 and both ER catabolic pathways.

3.3. Motor dysfunction in *Tor1a* KI/*Fbg1* KO mice

In this study, we identified mild, age-related motor deficits caused by genetic defects in the *Fbg1* and *Tor1a* genes. First, we found a rotarod deficit for the *Tor1a* KI mouse. This appears to be age-related, as a recent report does not describe abnormal rotarod performance in this mouse model up to 12 months of age (Tanabe et al., 2012). When each trial day was analyzed separately, as done by Jinnah and colleagues (Song et al., 2012), we found defective performance from day 1 as these authors did in younger mice. Our data also suggest the possibility of a motor learning defect (reduced performance at day 3) similar to a

previously reported age-related deficit in DYT1 transgenic mice (Sharma et al., 2005). But, why would the lack of FBG1 rescue this defect? A possibility is that the absence of FBG1 does not affect total torsinA levels but it does influence the torsinA(wt):(ΔE) ratio (there are no available antibodies that distinguish the wt from the mutant protein). Another possibility is that the absence of FBG1 leads to adaptive changes in the rodent brain that indirectly affect this phenotype. Nevertheless, these are purely speculative possibilities that will need to be addressed in future studies.

We also found hypoactive spontaneous locomotion caused by both the loss of FBG1 and the DYT1 mutation, similarly restricted to aged mice. This is in contrast to the reported hyperactivity in the other DYT1 models (Dang et al., 2005, Shashidharan et al., 2005, Grundmann et al., 2007). It should be pointed out that the significance of the age-related changes identified in these studies and by others is unclear, as DYT1 dystonia is a childhood onset disease.

Collectively with other reports, our experiments indicate the presence of subtle motor dysfunction in mouse models of DYT1 that is influenced by age, genetic background and probably experimental protocol and environment, among other factors. In fact, the influence of genetic background on survival was recently demonstrated in *Tor1a*$^{\Delta E/\Delta E}$ mice (Tanabe et al., 2012). Although the authors did not find that backcrossing to alternate strains induced rotarod or open field deficits up to 12 months of age, a recent publication of *Tor1a* KI mice in C57BL/6J background reported hyperactivity in *Tor1a* KI animals and impaired performance on the first day of rotarod testing (Song et al., 2012). A challenge for dystonia researchers will be to determine whether these phenotypes are a correlate of human dystonia, or if their underlying pathophysiology is different.

3.4. Conclusions

In summary, we show that FBG1 binds torsinA and reduces its expression levels in cultured cells. However, it is unlikely that FBG1 modifies DYT1 pathogenesis due to the presence of redundant catabolic pathways. Our findings also highlight the apparent molecular and functional versatility of the neuronal F-box protein FBG1 as another functional link between the UPP and autophagic pathways with potential implications for the pathogenesis of various neurological diseases. Finally, we add to previous publications indicating the development of mild motor dysfunction in aged DYT1 mice.

Acknowledgments

We thank all the members of the Gonzalez and Glenn laboratories for their helpful comments and Tom Moninger at the CMRF for assistance with microscopy. This work was funded by NIH (K02NS058450 to PGA, F31NS073348 to KLG and R01AG034228 to HLP) and VA Research Career Development Award 2006–12 (KAG).

Abbreviations

AP	alkaline phosphatase
ER	endoplasmic reticulum
ERAD	endoplasmic reticulum associated degradation
FBG1	F-box/G-domain protein 1
KI	knock in
KO	knock out
NGF	nerve growth factor

SCF	SKP, Cullin, F-box
UPP	ubiquitin proteasome pathway
3-MA	3-methyladenine

References

Arndt V, Dick N, Tawo R, Dreiseidler M, Wenzel D, Hesse M, Furst DO, Saftig P, Saint R, Fleischmann BK, Hoch M, Hohfeld J. Chaperone-assisted selective autophagy is essential for muscle maintenance. Current biology : CB. 2010; 20:143–148. [PubMed: 20060297]

Bai C, Sen P, Hofmann K, Ma L, Goebl M, Harper JW, Elledge SJ. SKP1 connects cell cycle regulators to the ubiquitin proteolysis machinery through a novel motif, the F-box. Cell. 1996; 86:263–274. [PubMed: 8706131]

Bernales S, McDonald KL, Walter P. Autophagy counterbalances endoplasmic reticulum expansion during the unfolded protein response. PLoS biology. 2006; 4:e423. [PubMed: 17132049]

Callan AC, Bunning S, Jones OT, High S, Swanton E. Biosynthesis of the dystonia- associated AAA+ ATPase torsinA at the endoplasmic reticulum. Biochem J. 2007; 401:607–612. [PubMed: 17037984]

Carra S, Seguin SJ, Lambert H, Landry J. HspB8 chaperone activity toward poly(Q)-containing proteins depends on its association with Bag3, a stimulator of macroautophagy. J Biol Chem. 2008; 283:1437–1444. [PubMed: 18006506]

Ciechanover A, Brundin P. The ubiquitin proteasome system in neurodegenerative diseases: sometimes the chicken, sometimes the egg. Neuron. 2003; 40:427–446. [PubMed: 14556719]

Crippa V, Sau D, Rusmini P, Boncoraglio A, Onesto E, Bolzoni E, Galbiati M, Fontana E, Marino M, Carra S, Bendotti C, De Biasi S, Poletti A. The small heat shock protein B8 (HspB8) promotes autophagic removal of misfolded proteins involved in amyotrophic lateral sclerosis (ALS). Hum Mol Genet. 2010; 19:3440–3456. [PubMed: 20570967]

Dang MT, Yokoi F, McNaught KS, Jengelley TA, Jackson T, Li J, Li Y. Generation and characterization of Dyt1 DeltaGAG knock-in mouse as a model for early-onset dystonia. Experimental neurology. 2005; 196:452–463. [PubMed: 16242683]

Erhardt JA, Hynicka W, DiBenedetto A, Shen N, Stone N, Paulson H, Pittman RN. A novel F box protein, NFB42, is highly enriched in neurons and induces growth arrest. J Biol Chem. 1998; 273:35222–35227. [PubMed: 9857061]

Gamerdinger M, Kaya AM, Wolfrum U, Clement AM, Behl C. BAG3 mediates chaperone-based aggresome-targeting and selective autophagy of misfolded proteins. EMBO reports. 2011; 12:149–156. [PubMed: 21252941]

Giles LM, Chen J, Li L, Chin LS. Dystonia-associated mutations cause premature degradation of torsinA protein and cell-type-specific mislocalization to the nuclear envelope. Hum Mol Genet. 2008; 17:2712–2722. [PubMed: 18552369]

Glenn KA, Nelson RF, Wen HM, Mallinger AJ, Paulson HL. Diversity in tissue expression, substrate binding, and SCF complex formation for a lectin family of ubiquitin ligases. J Biol Chem. 2008; 283:12717–12729. [PubMed: 18203720]

Gong B, Chen F, Pan Y, Arrieta-Cruz I, Yoshida Y, Haroutunian V, Pasinetti GM. SCFFbx2-E3-ligase-mediated degradation of BACE1 attenuates Alzheimer's disease amyloidosis and improves synaptic function. Aging cell. 2010; 9:1018–1031. [PubMed: 20854419]

Gonzalez-Alegre P, Bode N, Davidson BL, Paulson HL. Silencing primary dystonia: lentiviral-mediated RNA interference therapy for DYT1 dystonia. J Neurosci. 2005; 25:10502–10509. [PubMed: 16280588]

Gonzalez-Alegre P, Miller VM, Davidson BL, Paulson HL. Toward therapy for DYT1 dystonia: allele-specific silencing of mutant TorsinA. Ann Neurol. 2003; 53:781–787. [PubMed: 12783425]

Gonzalez-Alegre P, Paulson HL. Aberrant cellular behavior of mutant torsinA implicates nuclear envelope dysfunction in DYT1 dystonia. J Neurosci. 2004; 24:2593–2601. [PubMed: 15028751]

Goodchild RE, Dauer WT. Mislocalization to the nuclear envelope: an effect of the dystonia-causing torsinA mutation. Proc Natl Acad Sci U S A. 2004; 101:847–852. [PubMed: 14711988]

Goodchild RE, Kim CE, Dauer WT. Loss of the dystonia-associated protein torsinA selectively disrupts the neuronal nuclear envelope. Neuron. 2005; 48:923–932. [PubMed: 16364897]

Gordon KL, Glenn KA, Gonzalez-Alegre P. Exploring the influence of torsinA expression on protein quality control. Neurochemical research. 2011; 36:452–459. [PubMed: 21161590]

Gordon KL, Gonzalez-Alegre P. Consequences of the DYT1 mutation on torsinA oligomerization and degradation. Neuroscience. 2008; 157:588–595. [PubMed: 18940237]

Groisman B, Avezov E, Lederkremer GZ. The E3 Ubiquitin Ligases HRD1 and SCF^{Fbs2} Recognize the Protein Moiety and Sugar Chains, Respectively, of an ER-Associated Degradation Substrate. Israel Journal of Chemistry. 2006; 46:189–196.

Grundmann K, Reischmann B, Vanhoutte G, Hubener J, Teismann P, Hauser TK, Bonin M, Wilbertz J, Horn S, Nguyen HP, Kuhn M, Chanarat S, Wolburg H, Van der Linden A, Riess O. Overexpression of human wildtype torsinA and human DeltaGAG torsinA in a transgenic mouse model causes phenotypic abnormalities. Neurobiol Dis. 2007; 27:190–206. [PubMed: 17601741]

Hewett J, Gonzalez-Agosti C, Slater D, Ziefer P, Li S, Bergeron D, Jacoby DJ, Ozelius LJ, Ramesh V, Breakefield XO. Mutant torsinA, responsible for early-onset torsion dystonia, forms membrane inclusions in cultured neural cells. Hum Mol Genet. 2000; 9:1403–1413. [PubMed: 10814722]

Hewett JW, Nery FC, Niland B, Ge P, Tan P, Hadwiger P, Tannous BA, Sah DW, Breakefield XO. siRNA knock-down of mutant torsinA restores processing through secretory pathway in DYT1 dystonia cells. Hum Mol Genet. 2008; 17:1436–1445. [PubMed: 18258738]

Hewett JW, Tannous B, Niland BP, Nery FC, Zeng J, Li Y, Breakefield XO. Mutant torsinA interferes with protein processing through the secretory pathway in DYT1 dystonia cells. Proc Natl Acad Sci U S A. 2007; 104:7271–7276. [PubMed: 17428918]

Kato A, Rouach N, Nicoll RA, Bredt DS. Activity-dependent NMDA receptor degradation mediated by retrotranslocation and ubiquitination. Proc Natl Acad Sci U S A. 2005; 102:5600–5605. [PubMed: 15809437]

Koh YH, Rehfeld K, Ganetzky B. A Drosophila model of early onset torsion dystonia suggests impairment in TGF-beta signaling. Hum Mol Genet. 2004; 13:2019–2030. [PubMed: 15269177]

Kustedjo K, Bracey MH, Cravatt BF. Torsin A and its torsion dystonia-associated mutant forms are lumenal glycoproteins that exhibit distinct subcellular localizations. J Biol Chem. 2000; 275:27933–27939. [PubMed: 10871631]

Martin JN, Wolken N, Brown T, Dauer WT, Ehrlich ME, Gonzalez-Alegre P. Lethal toxicity caused by expression of shRNA in the mouse striatum: implications for therapeutic design. Gene therapy. 2011; 18:666–673. [PubMed: 21368900]

Misbahuddin A, Placzek MR, Taanman JW, Gschmeissner S, Schiavo G, Cooper JM, Warner TT. Mutant torsinA, which causes early-onset primary torsion dystonia, is redistributed to membranous structures enriched in vesicular monoamine transporter in cultured human SH-SY5Y cells. Mov Disord. 2005; 20:432–440. [PubMed: 15593317]

Murai-Takebe R, Noguchi T, Ogura T, Mikami T, Yanagi K, Inagaki K, Ohnishi H, Matozaki T, Kasuga M. Ubiquitination-mediated regulation of biosynthesis of the adhesion receptor SHPS-1 in response to endoplasmic reticulum stress. J Biol Chem. 2004; 279:11616–11625. [PubMed: 14701835]

Naismith TV, Heuser JE, Breakefield XO, Hanson PI. TorsinA in the nuclear envelope. Proc Natl Acad Sci U S A. 2004; 101:7612–7617. [PubMed: 15136718]

Nedelsky NB, Todd PK, Taylor JP. Autophagy and the ubiquitin-proteasome system: collaborators in neuroprotection. Biochim Biophys Acta. 2008; 1782:691–699. [PubMed: 18930136]

Nelson RF, Glenn KA, Miller VM, Wen H, Paulson HL. A novel route for F-box protein-mediated ubiquitination links CHIP to glycoprotein quality control. J Biol Chem. 2006; 281:20242–20251. [PubMed: 16682404]

Nelson RF, Glenn KA, Zhang Y, Wen H, Knutson T, Gouvion CM, Robinson BK, Zhou Z, Yang B, Smith RJ, Paulson HL. Selective cochlear degeneration in mice lacking the F-box protein, Fbx2, a glycoprotein-specific ubiquitin ligase subunit. J Neurosci. 2007; 27:5163–5171. [PubMed: 17494702]

Nery FC, Zeng J, Niland BP, Hewett J, Farley J, Irimia D, Li Y, Wiche G, Sonnenberg A, Breakefield XO. TorsinA binds the KASH domain of nesprins and participates in linkage between nuclear envelope and cytoskeleton. J Cell Sci. 2008; 121:3476–3486. [PubMed: 18827015]

O'Farrell CA, Martin KL, Hutton M, Delatycki MB, Cookson MR, Lockhart PJ. Mutant torsinA interacts with tyrosine hydroxylase in cultured cells. Neuroscience. 2009; 164:1127–1137. [PubMed: 19761814]

Olzmann JA, Li L, Chudaev MV, Chen J, Perez FA, Palmiter RD, Chin LS. Parkin-mediated K63-linked polyubiquitination targets misfolded DJ-1 to aggresomes via binding to HDAC6. J Cell Biol. 2007; 178:1025–1038. [PubMed: 17846173]

Ozelius LJ, Hewett JW, Page CE, Bressman SB, Kramer PL, Shalish C, de Leon D, Brin MF, Raymond D, Corey DP, Fahn S, Risch NJ, Buckler AJ, Gusella JF, Breakefield XO. The early-onset torsion dystonia gene (DYT1) encodes an ATP-binding protein. Nat Genet. 1997; 17:40–48. [PubMed: 9288096]

Pandey UB, Nie Z, Batlevi Y, McCray BA, Ritson GP, Nedelsky NB, Schwartz SL, DiProspero NA, Knight MA, Schuldiner O, Padmanabhan R, Hild M, Berry DL, Garza D, Hubbert CC, Yao TP, Baehrecke EH, Taylor JP. HDAC6 rescues neurodegeneration and provides an essential link between autophagy and the UPS. Nature. 2007; 447:859–863. [PubMed: 17568747]

Sharma N, Baxter MG, Petravicz J, Bragg DC, Schienda A, Standaert DG, Breakefield XO. Impaired motor learning in mice expressing torsinA with the DYT1 dystonia mutation. J Neurosci. 2005; 25:5351–5355. [PubMed: 15930383]

Shashidharan P, Sandu D, Potla U, Armata IA, Walker RH, McNaught KS, Weisz D, Sreenath T, Brin MF, Olanow CW. Transgenic mouse model of early-onset DYT1 dystonia. Hum Mol Genet. 2005; 14:125–133. [PubMed: 15548549]

Shimura H, Hattori N, Kubo S, Mizuno Y, Asakawa S, Minoshima S, Shimizu N, Iwai K, Chiba T, Tanaka K, Suzuki T. Familial Parkinson disease gene product, parkin, is a ubiquitin-protein ligase. Nat Genet. 2000; 25:302–305. [PubMed: 10888878]

Song CH, Fan X, Exeter CJ, Hess EJ, Jinnah HA. Functional analysis of dopaminergic systems in a DYT1 knock-in mouse model of dystonia. Neurobiol Dis. 2012

Tanabe LM, Martin C, Dauer WT. Genetic background modulates the phenotype of a mouse model of DYT1 dystonia. PLoS One. 2012; 7:e32245. [PubMed: 22393392]

Tarsy D, Simon DK. Dystonia. N Engl J Med. 2006; 355:818–829. [PubMed: 16928997]

Torres GE, Sweeney AL, Beaulieu JM, Shashidharan P, Caron MG. Effect of torsinA on membrane proteins reveals a loss of function and a dominant-negative phenotype of the dystonia-associated DeltaE-torsinA mutant. Proc Natl Acad Sci U S A. 2004; 101:15650–15655. [PubMed: 15505207]

Vander Heyden AB, Naismith TV, Snapp EL, Hanson PI. Static retention of the lumenal monotopic membrane protein torsinA in the endoplasmic reticulum. EMBO J. 2011; 30:3217–3231. [PubMed: 21785409]

Wen H, Kim N, Fuentes EJ, Mallinger A, Gonzalez-Alegre P, Glenn K. FBG1 is a promiscuous ubiquitin ligase that sequesters APC2 and causes S-phase arrest. Cell Cycle. 2010; 9:4506–4517. [PubMed: 21135578]

Yoshida Y, Chiba T, Tokunaga F, Kawasaki H, Iwai K, Suzuki T, Ito Y, Matsuoka K, Yoshida M, Tanaka K, Tai T. E3 ubiquitin ligase that recognizes sugar chains. Nature. 2002; 418:438–442. [PubMed: 12140560]

Yoshida Y, Murakami A, Iwai K, Tanaka K. A neural-specific F-box protein Fbs1 functions as a chaperone suppressing glycoprotein aggregation. J Biol Chem. 2007; 282:7137–7144. [PubMed: 17215248]

Highlights

- FBG1 promotes torsinA degradation
- FBG1 acts through both the proteasome and autophagy
- The N-terminal domain of FBG1 is key for its functional versatility
- Absence of FBG1 triggers age-related motor dysfunction in torsinA(ΔE) knock-in mice

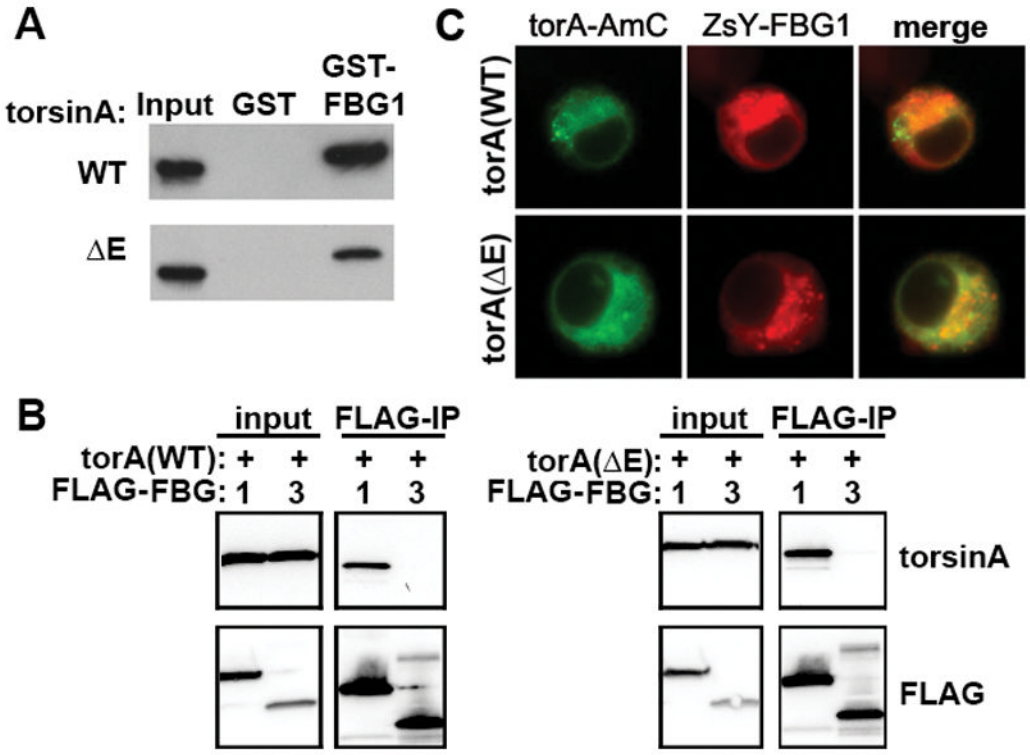

Figure 1. TorsinA and FBG1 physically interact

(A) Recombinant GST-FBG1 or GST control was incubated with lysates obtained from PC6.3 cells overexpressing torsinA(wt) or torsinA(ΔE) and GST complexes were pulled down using Glutathione-Sepharose-4B beads. Western blotting of the eluted precipitate was completed using anti-torsinA antibodies. (B) FLAG-FBG1 or FLAG-FBG3 as a control were transiently co-transfected with torsinA(wt) or torsinA(ΔE) in HEK293 cells, non-denaturing lysates were obtained 48 hrs later followed by immunoprecipitation with anti-FLAG affinity gel. Western blot analysis of the precipitate was completed for torsinA and FLAG. 10% Input and IP for each condition are from the same blot and the same exposure. Intervening lanes were excised for clarity. (C) Representative confocal images of PC6.3 cells cotransfected with torA(wt and ΔE)-AmCyan and ZsYellow-FBG1. Live cell images were taken 30 hours after transfection.

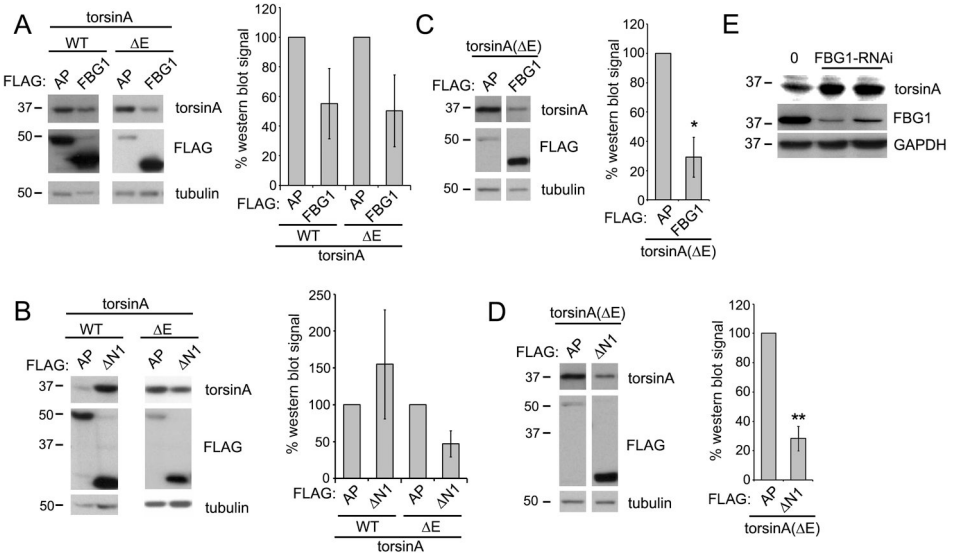

Figure 2. FBG1 and FBG1(ΔN) modulate torsinA levels in cultured cells

(A) Cos7 cells were co-transfected with torsinA(wt) or torsinA(ΔE) and FLAG-AP control or FLAG-FBG1. 48 hrs later protein lysates were obtained and western blot completed for torsinA, FLAG and α-tubulin expression. Shown are a representative blot and the quantification of 3 independent experiments. (B) Experiments completed as in (A) using FLAG-FBG1(ΔN) instead of FLAG-FBG1. (C) PC6.3 cells were co-transfected with torsinA(ΔE) and FLAG-FBG1, differentiated in NGF for 48 hrs after transfection and processed as in (A) and (B). (D) Experiments completed as in (C) using FLAG-FBG1(ΔN) instead of FLAG-FBG1. (E) Hep-G2 cells were transfected with shRNA #4306 to target endogenous FBG1. Cell lysates were obtained and western blot completed to detect expression of endogenous torsinA, FBG1 and GAPDH. A non-transfected and two transfected clones are shown. In all graphs, results are shown as mean ± SEM. Students t-test was performed to determine statistical significance (*/p≤0.05; **/p≤0.01). NGF: Nerve growth factor; CHX: cycloheximide; DOX: doxycycline; AP: alkaline phosphatase; ΔN1:FBG1(ΔN).

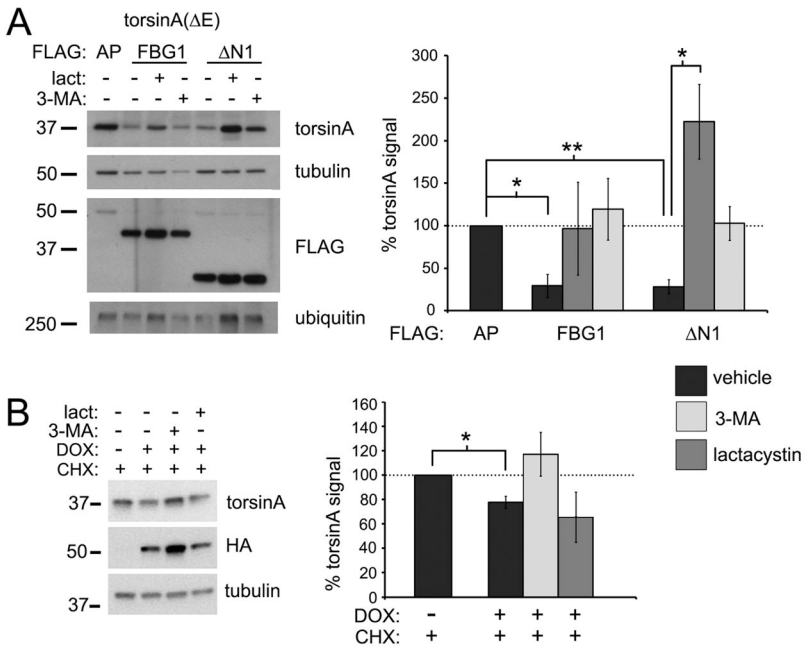

Figure 3. FBG1 reduces levels of torsinA by acting through the proteasome and autophagy

(A) PC6.3 cells were co-transfected with torsinA(ΔE) and FLAG-FBG1 or FLAG-FBG1(ΔN) and differentiated with NGF for 48 hrs. 10 mM 3-MA or 10 μM lactacystin were added for 12 hrs, protein lysates obtained and western blot completed to detect expression of torsinA, FLAG, ubiquitin and α-tubulin. Shown are a representative blot and the quantification of 3 independent experiments. Reference signal (100%) represents torsinA levels when co-transfected with FLAG-AP. (B) HA-FBG1-inducible PC6.3 cells were NGF-differentiated followed by induction of transgene expression with doxycycline as indicated. 10 mM 3-MA or 10 μM lactacystin and 10 μM cycloheximide were added for 24 hrs indicated. Western blot was completed for endogenous torsinA, HA and α-tubulin. Shown are a representative blot and the quantification of 3 independent experiments. Reference signal (100%) represents torsinA levels in the absence of HA-FBG1 induction. In all graphs, results are shown as mean ± SEM. Statistical analysis was performed using one-way ANOVA with Tukey's post hoc test. (*/p≤0.05, **/p≤0.01). Lact: lactacystin; 3-MA: 3-methyladenine; CHX: cycloheximide; DOX: doxycycline; AP: alkaline phosphatase; ΔN1: FBG1(ΔN).

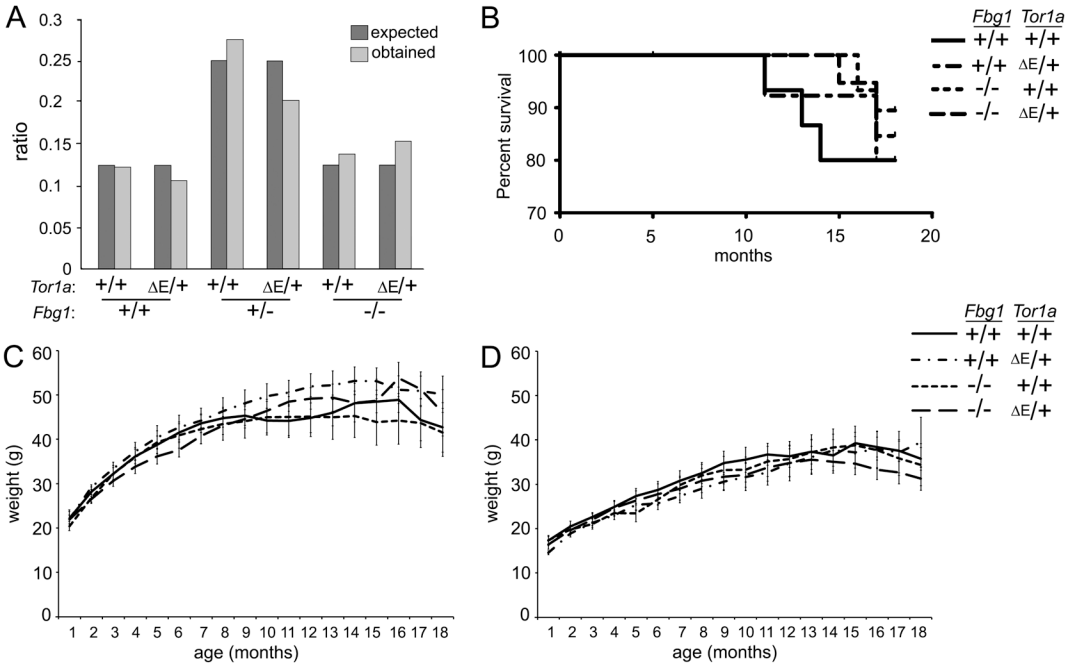

Figure 4. Mendelian ratios, survival, and weights are not influenced by loss of *Fbg1* in the torsinA(ΔE) knock-in mice

Tor1a$^{+/\Delta E}$-*Fbg1*$^{+/-}$ mice were bred generating a total of 123 animals. (A) Expected and obtained mendelian ratios for each genotype. (B) Kaplan-Meyer survival curve of the 4 experimental groups (*Tor1a*$^{+/\Delta E}$ or *Tor1a*$^{+/+}$ in *Fbg1*$^{+/+}$ or *Fbg1*$^{-/-}$ background). Monthly weights (mean ± SEM) for (C) males and (D) females surviving to 18 months were analyzed by repeated measures ANOVA. Number of animals for each genotype surviving to 18 months (male, female): *Fbg1*$^{+/+}$ *Tor1a*$^{+/+}$ (5, 7), *Fbg1*$^{+/+}$ *Tor1a*$^{+/\Delta E}$ (7, 4), *Fbg1*$^{-/-}$ *Tor1a*$^{+/+}$ (9, 3), *Fbg1*$^{-/-}$ *Tor1a*$^{+/\Delta E}$ (6, 11).

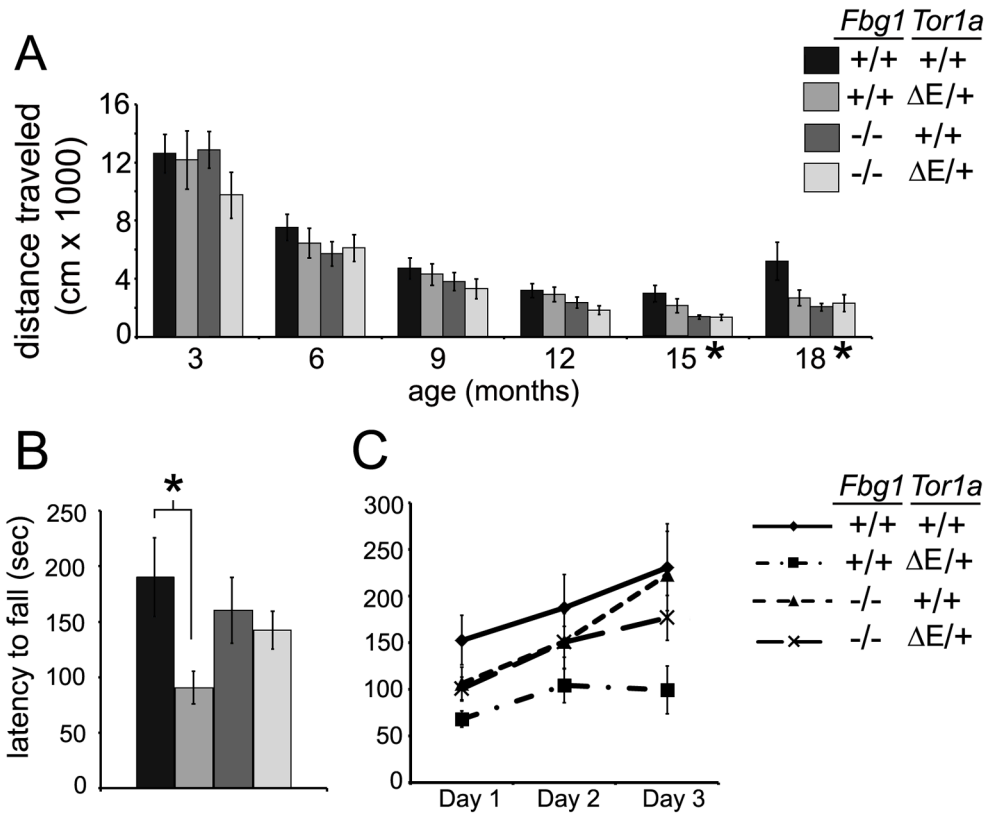

Figure 5. Motor phenotypes in *Tor1a*$^{+/\Delta E}$ and *Fbg1* KO mice

(A) Spontaneous locomotion was assessed by measuring the total distance traveled during a period of 90 minutes in an open field every 3 months. Mean ± SEM was calculated for each genotype. Repeated measures ANOVA was performed for mice surviving to 18 months. There was a significant effect of time ($F(4, 188) = 31.78$; $p<0.0001$) and genotype ($F(3, 47) = 2.87$; $p=0.0461$) on distance traveled, but no interaction. One way ANOVA was performed independently for each time point, demonstrating a significant difference (*) at 15 ($F(3, 47) = 4.059$; $p = 0.0120$) and 18 ($F(3, 47) = 3.389$; $p = 0.0256$) months. (B) Performance on the rotarod at 18 months is expressed as mean ± SEM latency to fall from 3 trials per day for 3 consecutive days. Results were analyzed by two-way ANOVA followed by Bonferroni post hoc test (*$p\leq0.05$). (C) Performance in the rotarod is shown for trial days 1–3. Repeated measures ANOVA showed a trend towards significance ($F(3, 37) = 2.62$; $p=0.0652$). When each day was analyzed individually, a significant effect of DYT1 genotype was present on days 1 ($F(1,37) = 6.35$; $p=0.0162$) and 3 ($F(1, 37) = 6.086$; $p= 0.0184$).

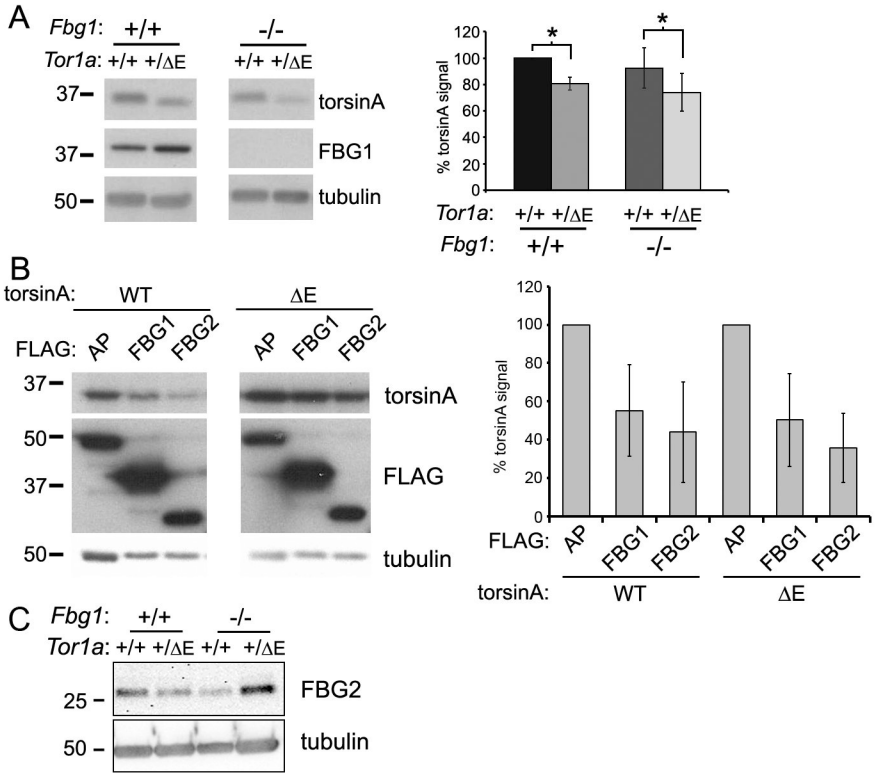

Figure 6. Absence of FBG1 does not alter neuronal torsinA levels *in vivo*.

(A) Mice were sacrificed at 18 months of age and their brains extracted. Whole brain protein lysates were obtained and western blot analysis completed (using 50 μg protein) to detect expression of torsinA, FBG1 and α-tubulin. Shown are a representative blot and the quantification of torsinA levels normalized to loading control (mean ± SEM) for 4 animals (2 males and 2 females). Two-way ANOVA was performed followed by Tukey's post hoc test (*/p≤0.05). (B) Cos7 cells were co-transfected with torsinA(wt) or torsinA(ΔE) and FLAG-AP control, FLAG-FBG1 or FLAG-FBG2. Protein lysates were obtained 48 hrs later and western blotting complete with torsinA, FLAG and α-tubulin antibodies. A representative blot and the quantification of 3 independent experiments are shown. One-way ANOVA was performed to determine statistical significance. (C) FBG2 expression was analyzed by western blot analysis from whole brain lysates (using 175 μg protein) as in (A).